Calculating fission rates at high spin: Incorporation of rotational degrees of freedom in thermodynamically fluctuating axially symmetric systems

J. P. Lestone*
Nuclear Physics Laboratory 354290, University of Washington, Seattle, Washington 98195
(Received 11 December 1997)

The methods presently used to calculate fission rates fail to correctly take into account the rotational degrees of freedom of compound nuclei rotating in three dimensions. The statistical model code JOANNE has been modified to correctly calculate the fission rates of classical thermodynamically fluctuating axially symmetric systems rotating in three dimensions. With this new code it is possible to reproduce evaporation residue cross sections, fission cross sections, and prescission neutron multiplicities from O-induced reactions, without the use of large fission delay times or large values of the viscosity of heated nuclear matter.
[S0556-2813(99)03103-9]

PACS number(s): 24.75.+i, 24.60.Ky, 25.70.Jj

Since the pioneering works of Holub *et al.* [1], Zank *et al.* [2], Gavron *et al.* [3,4], and Hinde *et al.* [5] showed that the standard theory of fission leads to an underestimation of measured prescission neutron multiplicities in heavy-ion reactions, much work has been done with the aim of better understanding why the standard model of fission fails. Most of this work has focused on the belief that the failure is somehow related to the viscosity of heated nuclear matter [6]. Few have considered the possibility that the problem is due to, or in part due to, an incorrect implementation of the standard model.

The Bohr-Wheeler theory [7] states that the fission decay width of a fully equilibrated system is

$$\Gamma_f = \frac{N_t}{2\pi D_i}, \tag{1}$$

where N_t is the number of transition states and D_i is the total level density of the initial system. By making several simplifying assumptions one can obtain what is generally referred to as the Bohr-Wheeler fission decay width

$$\Gamma_f = \frac{T}{2\pi}\exp\left(\frac{-B_f}{T}\right), \tag{2}$$

where B_f is the temperature dependent effective fission barrier height,

$$B_f = B_f(T=0) - \delta a T^2. \tag{3}$$

δa is the difference in the Fermi-gas level density parameters at the saddle point and the equilibrium position. This is the standard method of estimating fission decay rates in the statistical model codes CASCADE [8], ALERT [9], ALICE [10], PACE [11], JULIAN [12], and JOANNE [13].

Dynamical calculations of the fission rate using the Fokker-Planck equation [14] or the Langevin equation [15] give an asymptotic fission decay width of

$$\Gamma_f = \frac{\hbar\omega_{\rm eq}}{2\pi}\exp\left(\frac{-B_f}{T}\right)\left(\sqrt{1+\gamma^2}-\gamma\right), \tag{4}$$

where $\gamma = \beta/(2\omega_{\rm sp})$, β is the reduced nuclear dissipation coefficient, and $\omega_{\rm eq}$ and $\omega_{\rm sp}$ are the curvatures of the potential energy surface at the equilibrium position and the fission saddle point, respectively. The $(\sqrt{1+\gamma^2}-\gamma)$ term is commonly referred to as the Kramers reduction factor and is due to the slowing effects of nuclear dissipation. The factor in front of the exponential in Eq. (4) differs from that in Eq. (2) by $\hbar\omega_{\rm eq}/T$. The origin of this difference was first pointed out by Strutinsky [16] and is due to the fact that in obtaining Eq. (2) there is no summation over the possible shapes and momenta of the collective coordinate in obtaining the initial total level density.

However, Eq. (4) is not the full fission decay width, but the fission decay width for a system with fixed spin K about the symmetry (fission) axis. $B_f, \omega_{\rm eq}$, and $\omega_{\rm sp}$ should all be considered functions of K, and the fact that K is not a constant of the motion of the system needs to be taken into account before a correct expression for the fission decay width can be determined. To illustrate this problem, let us consider the two systems $J=0$ ^{238}U and $J=57$ ^{208}Pb, and assume that in both systems the level density parameter is independent of deformation, and that the viscosities and temperatures are the same. These $J=0$ ^{238}U and $J=57$ ^{208}Pb systems have approximately the same fission barrier heights and the same potential curvatures $\omega_{\rm eq}$ and $\omega_{\rm sp}$. Thus, according to Eq. (4) these two systems would have almost identical fission decay rates. This, however, cannot be the case because the low spin ^{238}U fission fragments will be emitted isotropically, while the high spin ^{208}Pb fragments will be seen only in directions close to the plane perpendicular to the total spin. This restriction in the possible direction in the ^{208}Pb fragments must be associated with a reduction in the number of fission transition states and therefore, given equal fission barrier heights and potential curvatures, the fission decay width of the high spin ^{208}Pb must be smaller than the decay width of the low spin ^{238}U.

This paradox is easily solved by labeling states by their orientation in space in addition to their shape and collective

*Present address: Los Alamos National Laboratory, Los Alamos, NM 87545.

momentum (kinetic energy). By assuming axially symmetric shapes, the sum over all possible orientations in space can be obtained by summing over all possible K from $K=-J$ to J, where J is the total spin and K is the projection of J onto the symmetry axis of the system. The Bohr-Wheeler fission decay width then becomes

$$\Gamma_f^{\mathrm{BW}}=\frac{\sum_K P(K)\Gamma_f^{\mathrm{BW}}(K)}{\sum_K P(K)}, \tag{5}$$

where $\Gamma_f^{\mathrm{BW}}(K)$ is the Bohr-Wheeler decay width as a function of K,

$$\Gamma_f^{\mathrm{BW}}(K)=\frac{\hbar\omega_{\mathrm{eq}}}{2\pi}\exp\left(\frac{-B_{\mathrm{f}}}{T}\right), \tag{6}$$

and $P(K)$ is the probability that the system is in a given K state,

$$P(K)=\frac{T}{\hbar\omega_{\mathrm{eq}}}\exp\left(\frac{-V_{\mathrm{eq}}}{T}\right). \tag{7}$$

V_{eq} is the sum of the Coulomb, nuclear, and rotational energies at the equilibrium position as a function of K.

To obtain an expression for the asymptotic fission decay width which includes the slowing effects of nuclear viscosity, the $\Gamma_f^{\mathrm{BW}}(K)$ term in Eq. (5) needs to be multiplied by the Kramers reduction factor. The above expressions were obtained assuming that the excitation energy is high enough that the temperature is the same at all the equilibrium positions and at all the fission saddle points. At lower excitation energies it becomes necessary to replace the temperature under the V_{eq} term by the temperature at the corresponding equilibrium position, T_{eq}, and to replace the temperature under the B_f term with the average of the nuclear temperatures at the corresponding equilibrium and saddle points, $(T_{\mathrm{eq}}+T_{\mathrm{sp}})/2$.

If $\omega_{\mathrm{eq}}, V_{\mathrm{eq}}$, and the shape of the fission saddle points are assumed to be independent of K, then Eq. (5) simplifies to

$$\Gamma_f^{\mathrm{BW}}=\Gamma_f^{\mathrm{BW}}(K=0)\,\frac{K_0\sqrt{2\pi}}{2J+1}\mathrm{erf}\left(\frac{J+1/2}{\sqrt{2}K_0}\right) \tag{8}$$

$$\sim\Gamma_f^{\mathrm{BW}}(K=0) \quad J\ll K_0 \tag{9}$$

$$\sim\Gamma_f^{\mathrm{BW}}(K=0)\frac{5K_0}{4J} \quad J\gg K_0, \tag{10}$$

where $K_0^2=TI_{\mathrm{eff}}^{\mathrm{sp}}/\hbar^2$. Here $I_{\mathrm{eff}}^{\mathrm{sp}}$ is the effective moment of inertia of the fission saddle point [17]. From Eq. (9) we see that at low spin the inclusion of the orientation degrees of freedom makes little difference to the fission decay width. At high spin the inclusion of the orientation degrees of freedom causes a reduction of the deduced decay width, with increasing spin, relative to the $K=0$ decay width. This reduction is easy to understand and is due to the time spent inside the fission saddle in configurations with the symmetry axis far from the plane perpendicular to the total spin. When in these $K\gg 0$ states the centrifugal forces associated with high spin collective rotation are reduced and thus the fission probability per unit time is lowered.

When solving for fission time scales using the Langevin equation, the acceleration of the fission coordinate q over a small time interval δt is given by [15]

$$\ddot{q}=-\frac{1}{\mu}\frac{\partial V}{\partial q}-\frac{\dot{q}^2}{2\mu}\frac{\partial\mu}{\partial q}-\beta\dot{q}+\Gamma\sqrt{\frac{2\beta T}{\delta t\mu}}, \tag{11}$$

where μ is the inertia of the collective coordinate q, and Γ is a random number from a normal distribution with unit variance. After a short relaxation time due to the equilibration of q with the nuclear heat bath, Eq. (11) leads to the asymptotic fission decay width as given by Eq. (4). As already pointed out, this equation is not the fission decay width but the decay width for a system with fixed K. This problem, with the standard Langevin description of fission, can be solved by calculating the potential energy surface as a function of both deformation q and the spin about the symmetry (fission) axis, K, and by treating K as a thermodynamically fluctuating overdamped coordinate. The amount by which K changes over a small time interval δt is then given by

$$\Delta K=-\frac{\delta t}{\gamma_K}\frac{\partial V}{\partial K}+\Gamma_K\sqrt{\frac{2T\delta t}{\gamma_K}}, \tag{12}$$

where γ_K is a parameter which controls the coupling between K and the nuclear heat bath. After a relaxation time associated with the equilibration of both q and K, Eq. (11) and Eq. (12), used in conjunction, lead to asymptotic fission decay widths which are in agreement with Eq. (5) with the $\Gamma_f^{\mathrm{BW}}(K)$ term multiplied by the Kramers reduction factor. All previous dynamical calculations of fission at high spin (see, for example, [18–20]) have failed to correctly treat the K degree of freedom and have thus overestimated the fission decay width at high spin. If γ_K as a function of q is chosen such that inside the fission saddle point the K relaxation time is short compared to the mean fission time, and if beyond the saddle point the K relaxation time is long compared to the saddle-to-scission transition time, then Eq. (11) and Eq. (12) give fission K distributions, and therefore fission fragment angular distributions, that are in agreement with the standard transition state model of fragment angular distributions [17].

The latest version of my statistical model code, JOANNE4, calculates fission decay widths using Eq. (5) with the modifications to the V_{eq}/T and B_f/T terms as discussed earlier. The potential energy surfaces V as a function of Z, A, J, K, q, and T were estimated using the expression [21]

$$V=S'(q)(1-\kappa T^2)E_S^0(Z,A)+C(q)0.7053\frac{Z^2}{A^{1/3}}\ \mathrm{MeV}$$
$$+\frac{[J(J+1)-K^2]\hbar^2}{I_\perp(q)\frac{4}{5}MR_0^2+8Ma^2}+\frac{K^2\hbar^2}{I_\parallel(q)\frac{4}{5}MR_0^2+8Ma^2}. \tag{13}$$

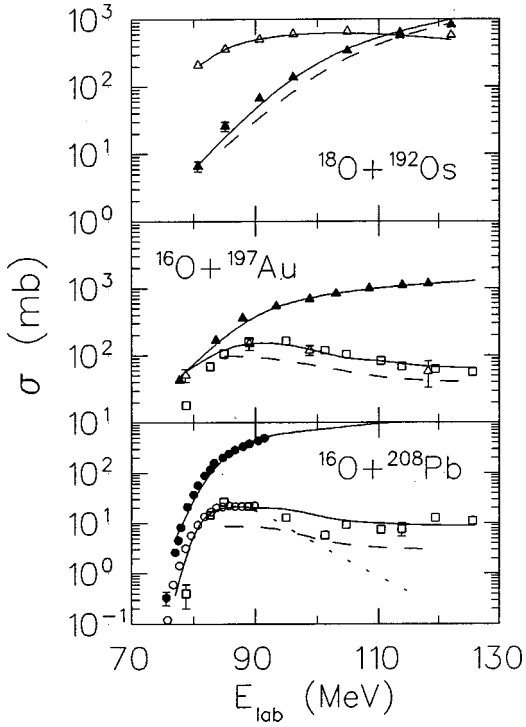

FIG. 1. Evaporation residue cross sections σ_{er} (open symbols) and fission cross sections σ_{fis} (solid symbols) as a function of the projectile energy for three O-induced reactions. The triangles, squares, and circles show the data of [5], [23], and [24], respectively. The dotted line shows a ''standard model'' calculation of the $^{16}O+^{208}Pb$ evaporation residue cross sections [22]. The dashed lines show JOANNE4 calculations with $\kappa=0$ and the solid lines with $\kappa=(0.007,\ -0.007,$ and $-0.011)$ MeV^{-2} for the reactions $^{18}O+^{192}Os$, $^{16}O+^{197}Au$, and $^{16}O+^{208}Pb$, respectively.

The $(1-\kappa T^2)$ term gives a temperature dependence to the potential energy surface. The statistical model codes CASCADE, ALERT, ALICE, PACE, JULIAN, and JOANNE have the adjustable parameters a_f/a_n and a barrier scaling term k_f which can be adjusted to reproduce low and moderate energy heavy-ion-induced evaporation residue cross sections and fission cross sections. In a similar fashion, the parameter κ can be adjusted to fit residue and fission cross sections using the new code JOANNE4. The parameter κ affects the temperature dependence of Γ_f and plays a role similar to a_f/a_n in other codes.

Measured σ_{er} and σ_{fis} for three heavy-ion reactions involving O projectiles are shown in Fig. 1. The dashed lines show model calculations performed using JOANNE4, with $\kappa=0$, a level density parameter $a_n=A/9$ MeV^{-1}, and Q values calculated using the experimental masses of the projectile and target and the liquid drop model masses of the initial compound systems. Notice that these $\kappa=0$ calculations underestimate the $^{16}O+^{208}Pb$ and $^{16}O+^{197}Au$ σ_{er} and underestimate the $^{18}O+^{192}Os$ σ_{fis}. This implies that the Th and Fr finite range droplet model fission barriers are too small and that the Po barriers are too high. This incorrect modeling of the σ_{er} and σ_{fis} has been removed by previous authors by either an arbitrary scaling of the fission barriers or the introduction of a_f/a_n values not equal to 1. Here I have chosen to use the parameter κ, which controls the temperature dependence of the potential energy surfaces. My reason for doing this is that an adjustment of the fission barriers (or a_f/a_n) also leads to a corresponding adjustment of the potential curvatures. The introduction of the parameter κ produces a simple self-consistent adjustment to both the barrier heights and potential curvatures as a function of both spin and temperature.

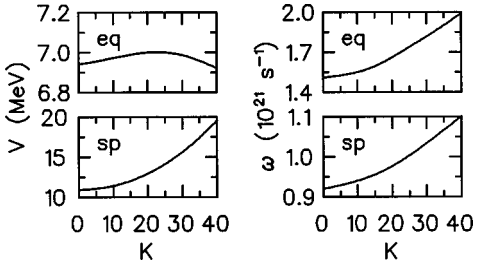

FIG. 2. $V_{eq}, V_{sp}=V_{eq}+B_f, \omega_{eq}$, and ω_{sp} for $T=0$, $J=40$, ^{213}Fr nuclei as a function of K.

The solid lines in Fig. 1 show JOANNE4 calculations with $\kappa=(0.007,\ -0.007,$ and $-0.011)$ MeV^{-2} for the reactions $^{18}O+^{192}Os$, $^{16}O+^{197}Au$, and $^{16}O+^{208}Pb$, respectively. Good quality fits to this data can also be obtained with $\kappa=0$ if the Th, Fr, and Po fission barriers are multiplied by the scaling factors 1.11, 1.07, and 0.93, respectively, or by introducting an a_f/a_n of 0.97, 0.98, and 1.02 for the Th, Fr, and Po systems, respectively. The ''standard model'' calculation (dotted line) of [22] fails to reproduce the high energy $^{16}O+^{208}Pb$ evaporation residue cross sections, while the JOANNE4 calculations give a much more satisfactory reproduction of the measured σ_{er} at the higher beam energies. Figure 2 shows $V_{eq}, V_{sp}=V_{eq}+B_f, \omega_{eq}$, and ω_{sp} for $T=0$, $J=40$, ^{213}Fr nuclei as a function of K. Figure 3 shows the temperature dependence of B_f for $K=0$, ^{210}Po nuclei at various J with $\kappa=0.007$ MeV^{-2}. For $T\lesssim 2$ MeV, saddle point shapes are insensitive to T, and thus B_f decrease linearly with T^2. This linear dependence of B_f on T^2 can be easily converted into a_f/a_n [see Eq. (3)]. Figure 4 shows a_f/a_n as a function of J for $K=0$ ^{224}Th, ^{213}Fr, and ^{210}Po with $\kappa=-0.011, -0.007$, and 0.007 MeV^{-2}, respectively.

In Fig. 5 JOANNE4 calculations of prescission neutron multiplicities ν_{pre} with $\kappa=0$ (solid lines) are compared to the corresponding measurements and to calculations where the fission decay widths were incorrectly calculated using Eq. (2) (dashed lines) instead of Eq. (5). A comparison of the dashed and solid curves clearly shows the increase in the calculated ν_{pre} obtained by switching from Eq. (3) to Eq. (5),

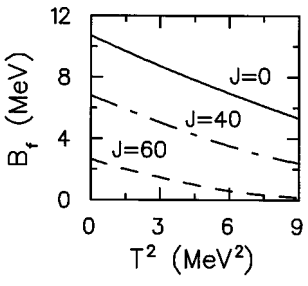

FIG. 3. B_f as a function of T^2 for $K=0$, ^{210}Po nuclei at various J with $\kappa=0.007$ MeV^{-2}.

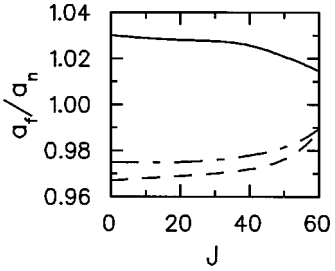

FIG. 4. a_f/a_n as a function of J for $K=0$ ^{224}Th (dashed line), ^{213}Fr (dash-dotted line), and ^{210}Po (solid line) with $\kappa=-0.011$, -0.007, and 0.007 MeV^{-2}, respectively.

while keeping all other model assumptions fixed. The calculations in Fig. 5 should not be used to draw conclusions about the presence of fission delay times or nuclear dissipation because the corresponding calculations of the $\sigma_{\rm er}$ and $\sigma_{\rm fis}$ fail to reproduce the cross section data shown in Fig. 1.

In Fig. 6 JOANNE4 calculations (solid lines) are compared to measured pre-scission neutron multiplicities, $\nu_{\rm pre}$. These calculations are with κ values that reproduce the corresponding $\sigma_{\rm er}$ and $\sigma_{\rm fis}$ data (see Fig. 1). These JOANNE4 model calculations give a reasonable reproduction of the $\nu_{\rm pre}$ data for the three O-induced reactions considered here. The dashed lines show the ''standard model'' calculations of others [5,22], which fail to reproduce the $\nu_{\rm pre}$ data. The dashed curves in Fig. 6 differ slightly from the dashed curves in Fig. 5, because in obtaining the dashed curves shown in Fig. 6 the authors [5,22] used fission barrier scaling factors and a_f/a_n values that gave a good reproduction of the corresponding $\sigma_{\rm er}$ and $\sigma_{\rm fis}$ data. A ''standard model'' analysis of the data considered here and other similar data and the analysis of gamma rays from heavy-ion fission reactions have led many

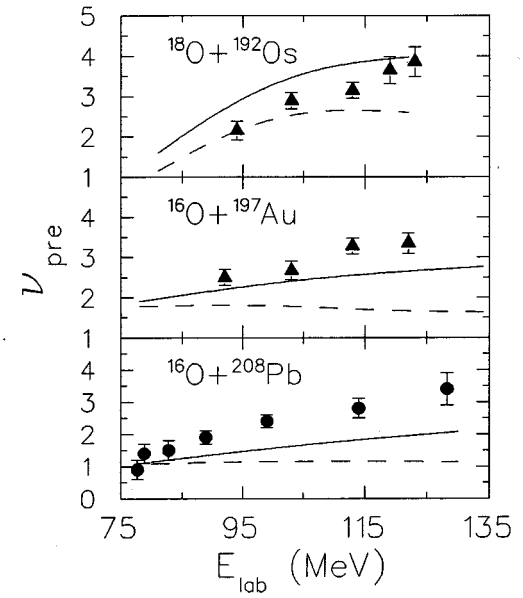

FIG. 5. Prescission neutron multiplicities $\nu_{\rm pre}$ as a function of the projectile energy for three O-induced reactions. The triangles and circles show the data of [5] and [30], respectively. The solid curves show JOANNE4 calculations with $\kappa=0$. The dashed curves show the same calculations but with the fission decay widths incorrectly calculated using Eq. (2) instead of Eq. (5).

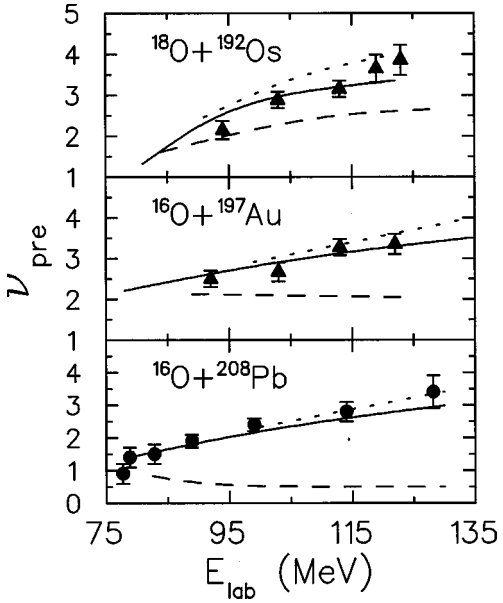

FIG. 6. Prescission neutron multiplicities $\nu_{\rm pre}$ as a function of the projectile energy for three O-induced reactions. The triangles and circles show the data of [5] and [30], respectively. The dashed lines show the ''standard model'' calculations of others [5,22]. The solid lines show calculations of $\nu_{\rm pre}$ obtained using JOANNE4 with no dynamical fission delay time and with κ values that reproduce the corresponding $\sigma_{\rm er}$ and $\sigma_{\rm fis}$ data (see Fig. 1). The dotted lines show JOANNE4 calculations where the particle emission from the equilibrium position is allowed to continue for an additional 3×10^{-20} s after the decision to fission has been made.

to conclude large dynamical fission time scales [5,25,26], large values of the viscosity of heated nuclear matter [27,28], a strong temperature dependence of the nuclear viscosity [22,28], and a strong deformation dependence of the nuclear viscosity [29]. It has therefore become generally accepted that the motion of heated nuclear matter along the path to fission is overdamped [6,28]. The dotted lines in Fig. 6 show JOANNE4 model calculations, similar to the solid curves, but with the particle emission from the equilibrium position allowed to continue for an additional 3×10^{-20} s after the decision to fission has been made. These calculations estimate the increase in $\nu_{\rm pre}$ expected from a presaddle fission delay $\tau_{\rm pre}$ and a saddle-to-scission transition time $\tau_{\rm ssc}$, which sum to $\sim3\times10^{-20}$ s. Notice the insensitivity of these calculations to the introduction of the fission delay time. JOANNE4 calculations of $\nu_{\rm pre}$ become more sensitive to a dynamical fission delay time at higher beam energies or with more symmetric entrance channels, where the spins are higher and thus the mean fission times are lower.

Although the data considered here are consistent with the Bohr-Wheeler fission decay width as given in Eq. (5) with no fission delay, they do not rule out modest values of the viscosity or a fission delay time of $\lesssim3\times10^{-20}$ s. An equally good reproduction of the data shown in Fig. 1 and Fig. 6 can be obtained with Eq. (5) modified by the Kramers reduction factor. For example, if β is assumed to be 2×10^{21} s^{-1}, then one obtains ^{16}O+^{208}Pb $\sigma_{\rm er}$ and $\nu_{\rm pre}$ very similar to the solid lines shown in Fig. 1 and Fig. 6, if κ is chosen to be $+0.002$ MeV^{-2}. This value of κ corresponds to $a_f/a_n=1.006$ for low spin ^{224}Th nuclei instead of the a_f/a_n

$=0.967$ shown in Fig. 4. From the JOANNE4 calculations presented here I conclude that in O-induced fusion-fission reactions, with initial excitation energies $\lesssim 80$ MeV, the ν_{pre} data are consistent with the fission of fully equilibrated systems and that the collective motion in the fission degree of freedom is not necessarily strongly overdamped, in contradiction with the conclusions drawn by others.

In summary, the present standard methods used to calculate fission decay widths fail to correctly take into account the orientation degrees of freedom of compound nuclei rotating in three dimensions. If the effects of the orientation degrees of freedom as discussed in this paper are incorporated into model calculations, then the $\sigma_{er}, \sigma_{fis}$, and ν_{pre} data from the O-induced reactions considered here can be satisfactorily reproduced without the use of large fission delay times, large values of the nuclear viscosity, or strong temperature or deformation dependences of the viscosity of heated nuclear matter. Many previously deduced properties of the viscosity of nuclear matter should be viewed with caution. The large volume of heavy-ion-induced fission data measured over the past decade, with the aim of deducing the properties of nuclear viscosity, needs to be reanalyzed using the concepts discussed in this paper.

This work was supported in part by the U.S. Department of Energy.

[1] E. Holub *et al.*, Phys. Rev. C **28**, 252 (1983).
[2] W. P. Zank *et al.*, Phys. Rev. C **33**, 519 (1986).
[3] A. Gavron *et al.*, Phys. Lett. B **176**, 312 (1986).
[4] A. Gavron *et al.*, Phys. Rev. C **35**, 579 (1987).
[5] D. J. Hinde *et al.*, Nucl. Phys. **A452**, 550 (1986).
[6] D. Hilscher and H. Rossner, Ann. Phys. (Paris) **17**, 471 (1992).
[7] N. Bohr and J. A. Wheeler, Phys. Rev. **53**, 426 (1939).
[8] F. Pulnhofer, Nucl. Phys. **A280**, 267 (1977).
[9] M. Blann and T. A. Komoto, Lawrence Livermore National Laboratory Report No. UCID 19390, 1932.
[10] M. Blann and J. Bisplinghoff, Lawrence Livermore National Laboratory Report No. UCID 19614, 1983.
[11] A. Gavron, Phys. Rev. C **21**, 230 (1980).
[12] H. Rossner *et al.*, Phys. Rev. C **40**, 2629 (1989).
[13] J. P. Lestone *et al.*, Nucl. Phys. **A559**, 277 (1993).
[14] H. A. Kramers, Physica (The Hague) **7**, 284 (1940).
[15] D. Boilley *et al.*, Nucl. Phys. **A556**, 67 (1993).
[16] V. M. Strutinsky, Phys. Lett. **47B**, 121 (1973).
[17] R. Vandenbosch and J. R. Huizenga, *Nuclear Fission* (Academic Press, New York, 1973).
[18] G. R. Tillack *et al.*, Phys. Lett. B **296**, 296 (1992).
[19] Y. Abe *et al.*, Phys. Rep. **275**, 49 (1996).
[20] P. Fröbrich and I. I. Gontchar, Phys. Rep. **292**, 131 (1998).
[21] J. P. Lestone, Phys. Rev. C **51**, 580 (1995).
[22] D. J. Hofman *et al.*, Phys. Rev. C **51**, 2597 (1995).
[23] K. T. Brinkmann *et al.*, Phys. Rev. C **50**, 309 (1994).
[24] C. R. Morton *et al.*, Phys. Rev. C **52**, 243 (1995).
[25] D. J. Hinde *et al.*, Phys. Rev. C **39**, 2268 (1989).
[26] D. J. Hinde *et al.*, Phys. Rev. C **45**, 1229 (1992).
[27] R. Butsch *et al.*, Phys. Rev. C **44**, 1515 (1992).
[28] P. Paul and M. Thoennessen, Annu. Rev. Nucl. Part. Sci. **44**, 65 (1994).
[29] P. Fröbrich, I. I. Gontchar, and N. D. Mavlitov, Nucl. Phys. **A556**, 281 (1993).
[30] H. Rossner *et al.*, Phys. Rev. C **45**, 719 (1992).